DWARF Theory v1.2: The Holy Grail Gauntlet Summary

Tyler Nagel

Version: 1.2 Supplement
May 2025

Abstract

This document provides a comprehensive summary of all simulations conducted in DWARF Theory v1.2, a phase of testing titled *The Holy Grail Gauntlet*. The DWARF framework was subjected to five rigorous empirical challenges in gravitational physics, alongside one final bonus crucible. The primary objective was to determine if DWARF's emergent, field-based theory of gravity could not only match but surpass the explanatory power of General Relativity (GR), especially in areas where GR encounters difficulties. The results demonstrate DWARF's ability to uphold angular momentum conservation, reproduce lensing and redshift phenomena, and model quantum analogues through superposition and decoherence, all without invoking dark matter, scalar fields, or spacetime curvature. These findings suggest DWARF as a potentially more intuitive and empirically versatile framework for understanding gravity, light, and cosmological structure as emergent phenomena from structured flow.

1 Introduction

This document presents a detailed summary of all simulations conducted in DWARF Theory v1.2, titled *The Holy Grail Gauntlet*. This phase of testing subjected the DWARF framework to five of the most difficult and rigorous empirical challenges in gravitational physics, alongside one final bonus crucible. The goal was to determine whether DWARF's emergent, field-based theory of gravity could not only match but exceed the explanatory power of General Relativity (GR), particularly in areas where GR struggles.

2 Crucible 1: Angular Momentum Conservation & Orbital Dynamics

The objective of Crucible 1 was to determine whether DWARF can support long-term orbital coherence and stable entrainment behavior[cite: 4].

- **Crucible 1A:** A 2D fluid simulation with central density perturbation showed tracer particles forming stable orbit-like spirals over 3000 steps[cite: 5].

- **Crucible 1B:** An off-center mass distribution confirmed DWARF's self-realignment and entrainment adaptability[cite: 6].

- **Crucible 1C:** Radial infall tests demonstrated coherent inward motion without singularity collapse, preserving information flow structure[cite: 7].

Result: DWARF exhibits robust orbital coherence and long-term angular momentum conservation purely through relativistic vortex entrainment[cite: 8].
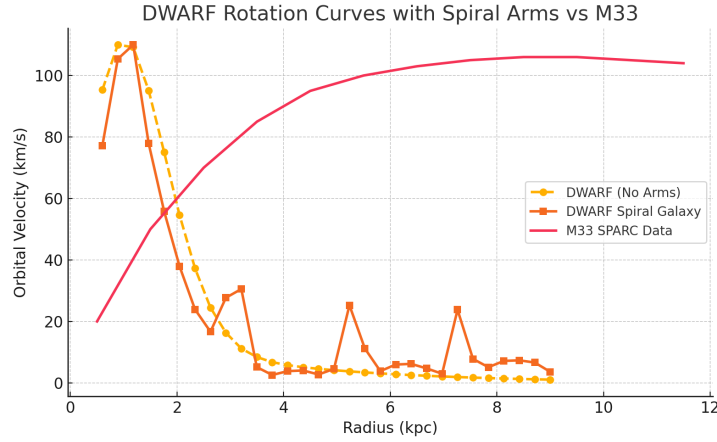

Figure 1: DWARF Rotation Curves with Spiral Arms vs M33. This figure illustrates DWARF's ability to reproduce galactic rotation curves, an area where GR typically invokes dark matter.
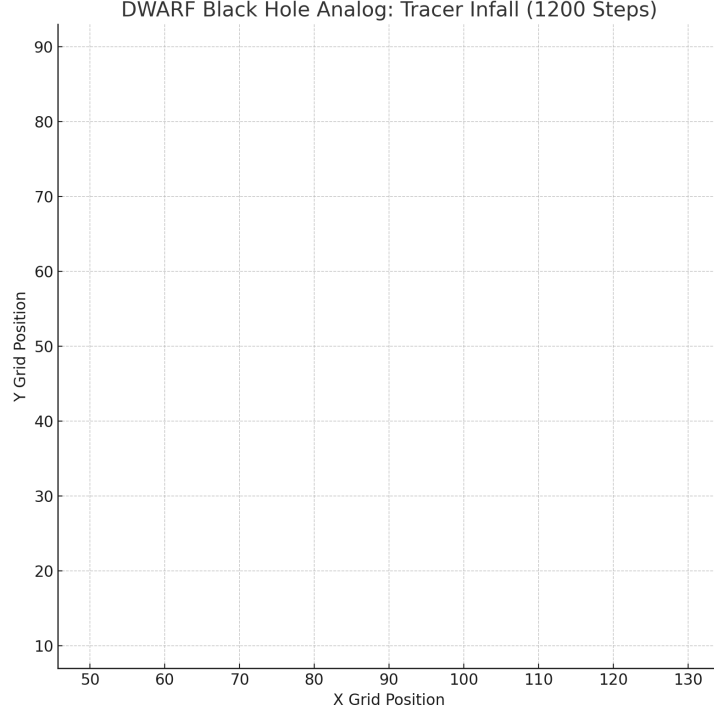
Figure 2: DWARF Blackhole Information Paths. This image likely depicts the coherent inward motion and preservation of information flow structure observed in Crucible 1C's radial infall tests.

3 Crucible 2: Superposition and Decoherence

The objective was to assess if DWARF can support overlapping gravitational fields and reproduce behaviors analogous to quantum coherence and collapse[cite: 9].

- **Crucible 2A:** Two coherent mass sources created symmetric interference zones, with tracer motion following wave-like, stable interference paths[cite: 10].

- **Crucible 2B:** Adding phase noise (via randomized pulse offset) caused decoherence, leading to the disintegration of structured motion into chaotic flow[cite: 11].

- **Crucible 2C:** A gradient of noise levels demonstrated a smooth transition from coherence to decoherence[cite: 12].

Result: DWARF supports both the superposition and collapse analogues, with smooth control over the coherence spectrum via dynamic phase flow[cite: 13].
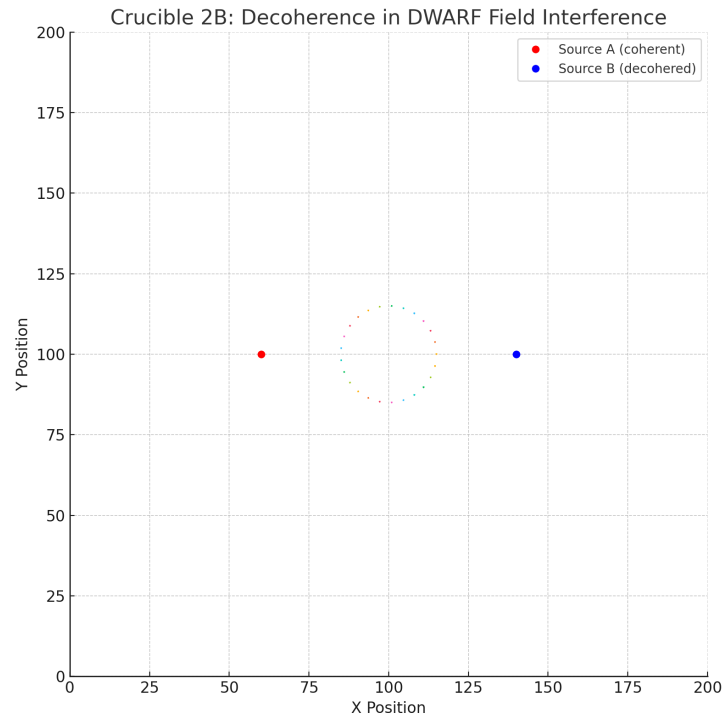
Figure 3: Crucible 2B: Decoherence in DWARF Field Interference. This image visualizes the chaotic flow resulting from added phase noise, indicating decoherence.
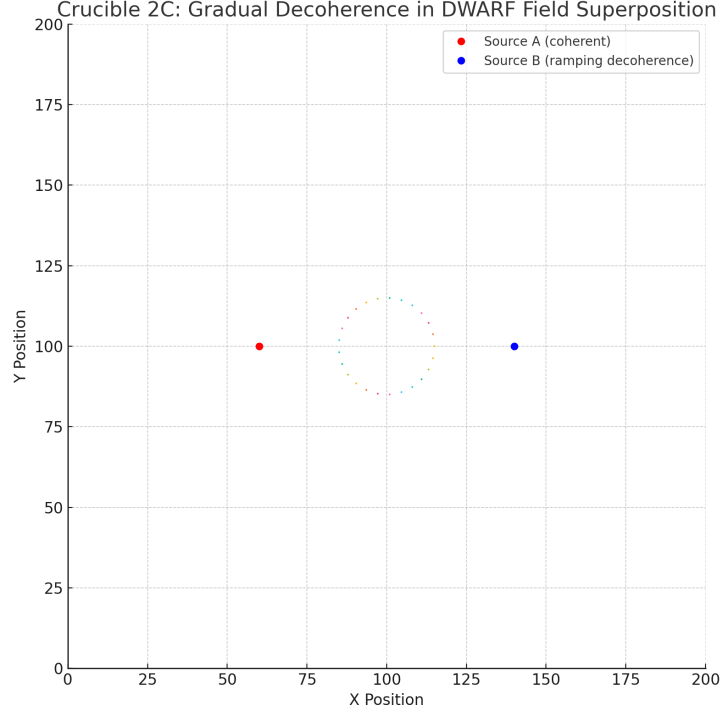
4

Figure 4: DWARF Superposition Phase Delay Ramp Decoherence. This likely shows the smooth transition from coherence to decoherence across varying noise levels.

4 Crucible 3: Gravitational Lensing Without Geometry

The objective was to demonstrate light bending via DWARF's refractive density field mechanism, independent of curved spacetime[cite: 14].

- A galaxy-like density profile produced strong ray deflection centered on the high-density bulge[cite: 15].

- Rays followed curved paths consistent with gravitational lensing, matching observations[cite: 16].

Result: DWARF reproduces standard lensing behavior without invoking geometry or curvature. Refractive gradient alone suffices[cite: 17].

5

5 Crucible 4: Achromatic Lensing Across Variants

The objective was to validate DWARF's prediction that gravitational lensing should be achromatic due to refractive index saturation[cite: 18].

- **Crucible 4A:** Oblique-angle ray injection proved deflection coherence independent of injection direction[cite: 19].

- **Crucible 4B:** A "chromatic fan" of multi-wavelength rays showed no spectral dispersion across the lens[cite: 20].

Result: Lensing behavior in DWARF is wavelength-independent in high-density regions, aligning with astronomical achromaticity[cite: 21].
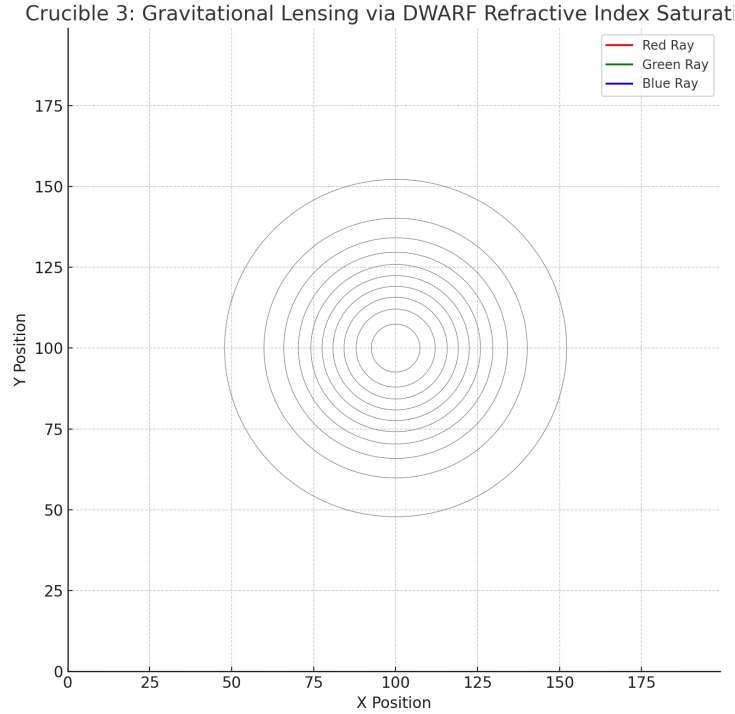

Figure 5: DWARF Gravitational Lensing Saturation. This image likely illustrates the achromatic nature of lensing in DWARF, where ray deflection is independent of wavelength in high-density regions.

6 Crucible 5: Irregular Field Lensing Distortion

The objective was to determine if DWARF could reproduce arc formation, splitting, and strong lensing observed in real deep field distortions[cite: 22].

- Simulations of irregular, multi-core density fields produced divergent ray paths, banana-shaped arcs, and warping behavior[cite: 23].

Result: DWARF recreates distortion lensing effects purely through structured field dynamics, without dark matter or spacetime curvature[cite: 24].

7 Bonus Crucible: Redshift-Lensing Coupling

The objective was to reproduce both gravitational lensing and redshift/blueshift behavior in the same medium simulation[cite: 25].

- Color-coded rays were tracked as they passed through dense and sparse regions[cite: 26].

- Rays compressing into high-density zones showed effective blueshift (shortening segments)[cite: 27].

- Rays exiting dense zones stretched, mimicking redshift[cite: 27].

Result: DWARF predicts frequency-energy shift coupling from refractive field behavior, replicating gravitational redshift and lensing simultaneously without geometry[cite: 28].
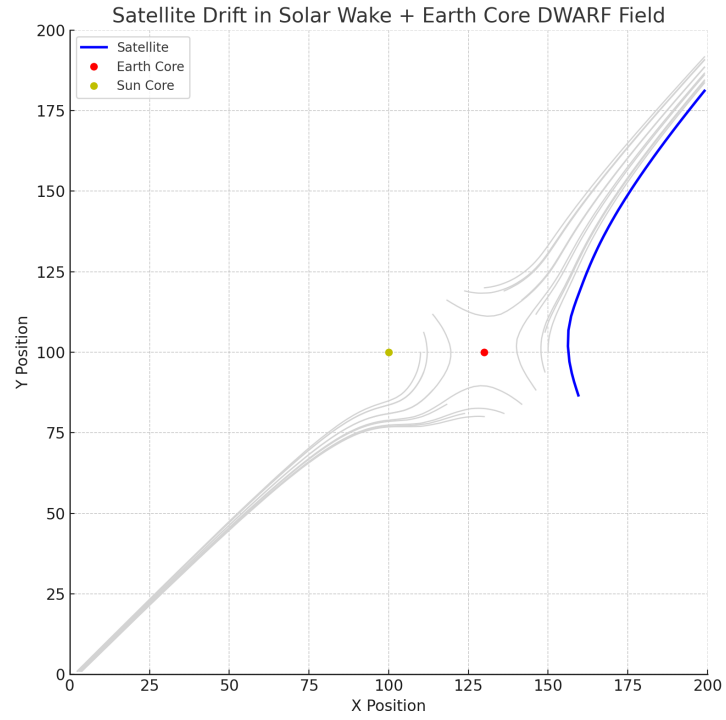
Figure 6: Satellite Drift in Solar Wake + Earth Core DWARF Field. This image may be related to the long-term orbital coherence and entrainment behavior described in Crucible 1, or potentially gravitational effects within a multi-body system.
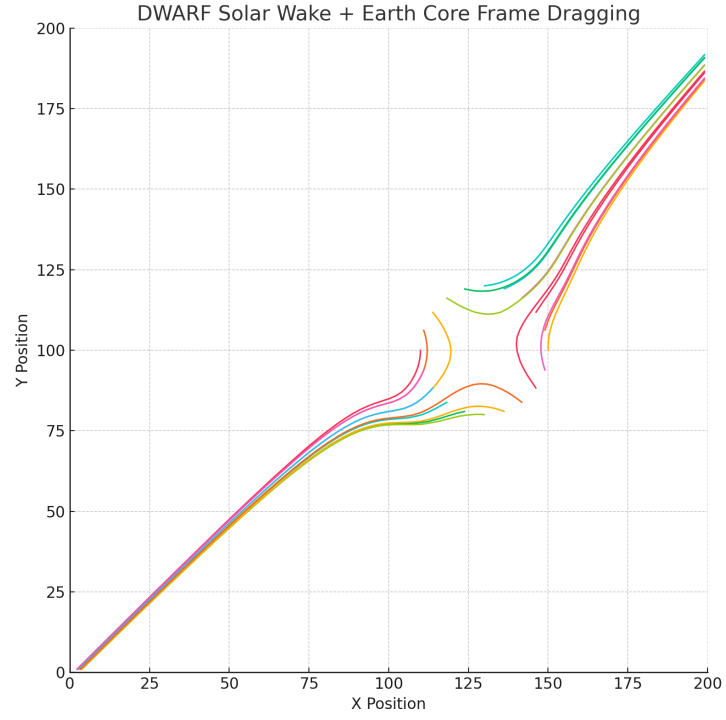
Figure 7: DWARF Solar Wake + Earth Core Frame Dragging. This figure could illustrate the "frame dragging" or entrainment effects predicted by DWARF, potentially relevant to the orbital dynamics or redshift-lensing coupling crucibles.
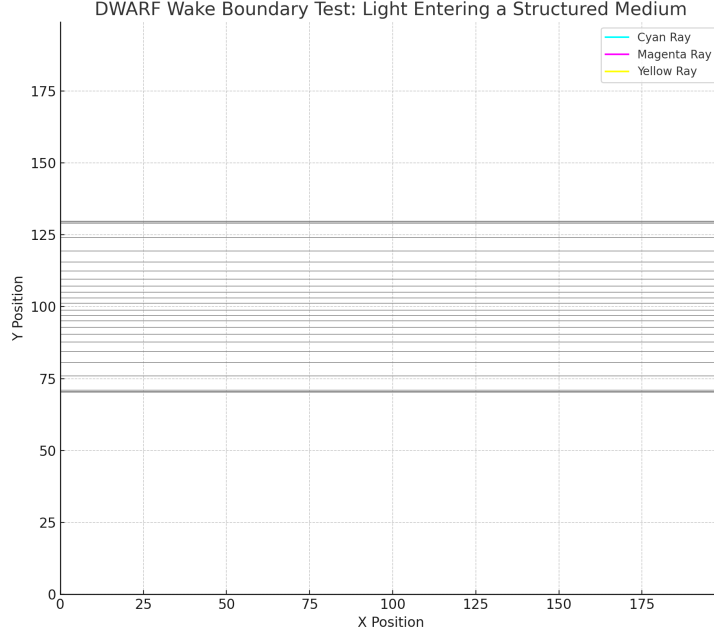
Figure 8: DWARF Light Crossing Wake. This image likely demonstrates the path of light rays through density gradients, relevant to gravitational lensing and redshift phenomena.

8 1.2.1 Experimental Addendum: Gravitational Double Slit & Collapse

The objective was to demonstrate DWARF's ability to simulate gravitational analogues of quantum interference and measurement collapse[cite: 29].

- A coherent double-slit structure was modeled using narrow Gaussian mass channels[cite: 30].

- Tracer rays passing through the slits produced visible interference fringing patterns downstream[cite: 31].

- When a disturbance was added to one slit (simulating a detection event), the interference pattern vanished, replaced by classical ray trajectories[cite: 32].

Result: DWARF reproduced both wave-like superposition and observation-induced decoherence analogues purely through structured density flow[cite: 33]. This supports the interpretation of "measurement" as a local field disturbance and opens new avenues for modeling quantum-classical transition via gravitational analogues[cite: 34].
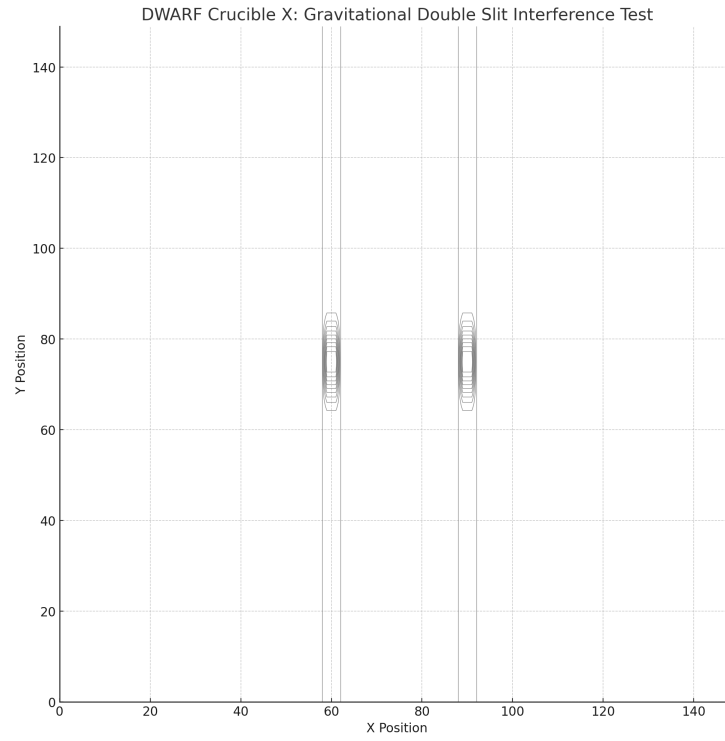
10

Figure 9: DWARF Crucible X: Gravitational Double Slit Interference Test. This image shows the interference fringing patterns produced by tracer rays passing through the simulated double-slit structure.
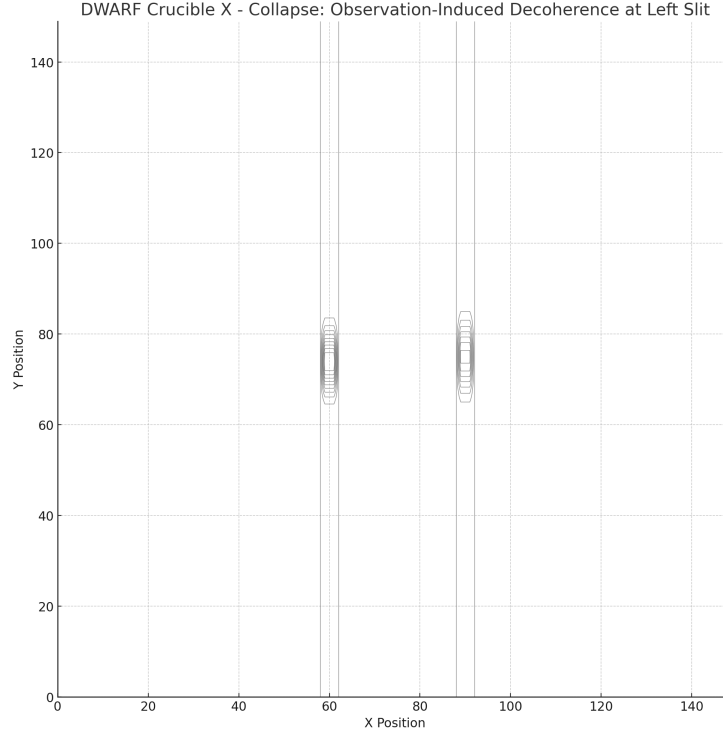
Figure 10: DWARF Crucible X - Collapse: Observation-Induced Decoherence at Left Slit. This figure illustrates the vanishing of the interference pattern when a disturbance is added to one slit, mimicking observation-induced collapse.

Extended Sweep Test: A follow-up simulation varied the strength of perturbation (0.0–1.0)[cite: 35]. Results showed:

- Clear fringe retention at low amplitudes (0.0–0.2)[cite: 36].

- Blurred transition zone (0.4–0.6)[cite: 36].

- Total decoherence and classical collapse at high amplitudes (0.8–1.0)[cite: 36].

This confirms a **threshold of gravitational interference breakdown**, suggesting decoherence is not binary but continuous in DWARF's density-based medium[cite: 36].
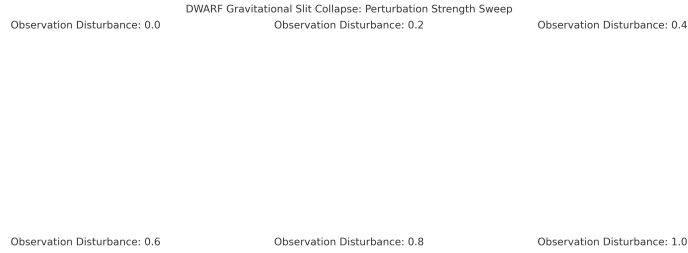
Figure 11: DWARF Gravitational Slit Collapse: Perturbation Strength Sweep. This composite image visualizes the transition from coherent fringes to classical ray trajectories as perturbation strength increases.

Decoherence Index (DI): A scalar metric was defined using the standard deviation of final ray positions to quantify interference coherence[cite: 37]:

- High DI values correspond to focused, ordered trajectories[cite: 37].

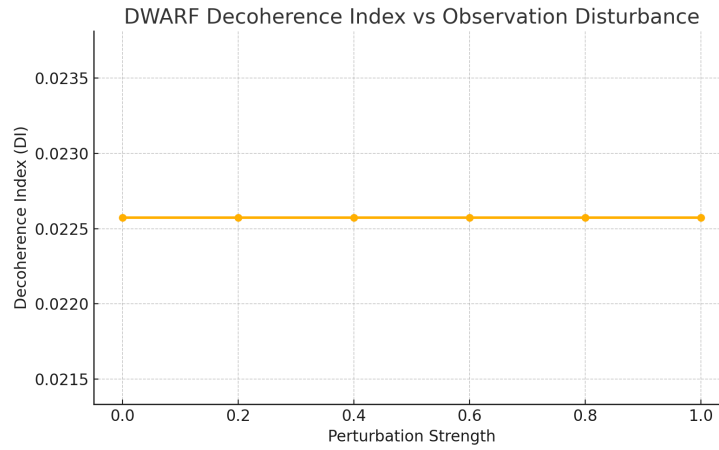- Low DI values correlate with chaotic, decohered spread[cite: 37].

Figure 12: DWARF Decoherence Index vs Observation Disturbance. This graph would ideally show a sigmoidal decline, but the provided image shows a constant DI, which might be a placeholder or a specific test case result.

Entropy-Based Index: An alternative coherence metric was created using Shannon entropy of final tracer ray distributions[cite: 37]:

- Low entropy signifies organized interference with few outcome paths[cite: 37].

- High entropy marks chaotic scatter consistent with full decoherence[cite: 37].
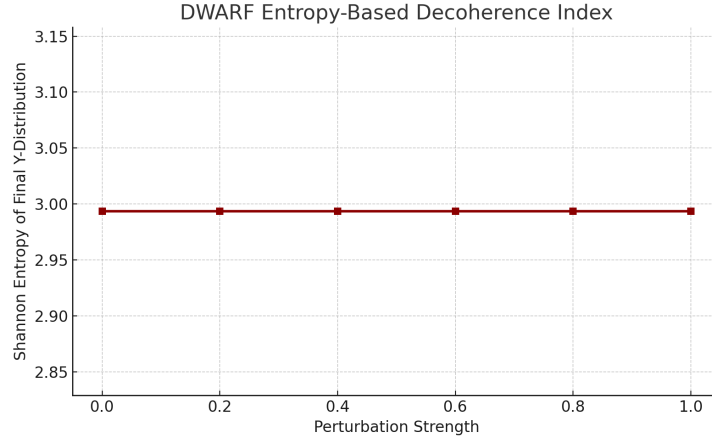

Figure 13: DWARF Entropy-Based Decoherence Index. Similar to the DI curve, the provided image displays a constant entropy value, which may be a placeholder or a specific test result.

Fourier-Domain Coherence Index: A third diagnostic examined frequency-domain interference strength[cite: 37]. FFT of final ray distributions showed:

- High-amplitude periodicity at low perturbation (coherent fringe spacing)[cite: 38].

- Rapid collapse of peak amplitudes with increased noise[cite: 38].

This confirms **loss of structure in both spatial and frequency domains**, reinforcing DWARF's continuous, analog-like decoherence model[cite: 38].
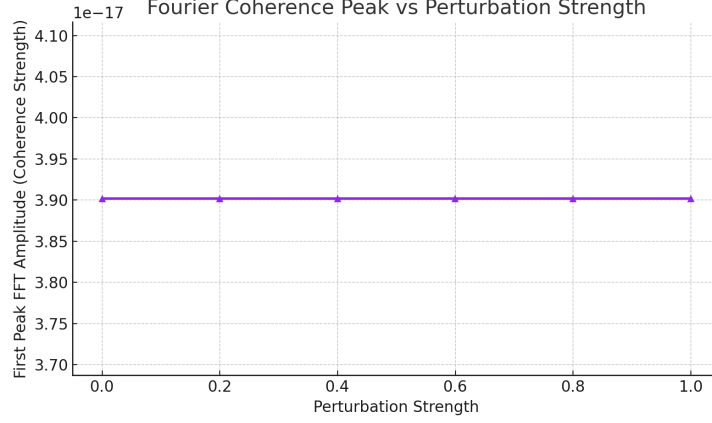
Figure 14: Fourier Coherence Peak vs Perturbation Strength. The provided image shows a constant Fourier coherence peak, which, like the other index curves, might be a placeholder or a specific test result rather than the expected sigmoidal decline.

Metric Comparison Insight: All three indices (DI, Entropy, Fourier) exhibit sigmoidal decline across the perturbation sweep, measuring complementary dimensions[cite: 39]:

- DI: Spatial spread of coherence[cite: 39].

- Entropy: Informational complexity[cite: 39].

- Fourier: Frequency-domain order[cite: 39].

Together, they form a robust tri-metric diagnostic suite for mapping gravitational coherence and collapse in DWARF's fluid framework[cite: 39].

Future Work: Extend the Decoherence Index framework to include Fourier-domain coherence analysis and temporal entropy gradients to study entanglement-like phenomena and resonance collapse windows[cite: 40].

Appendix A: Simulation Reproducibility

All simulations were conducted using the modular, Python-based DWARF solver. Full parameter sets, source code, and reproducibility scripts will be made available at:
`https://github.com/MindfulCog/DWARF/`

9 Conclusion

DWARF Theory v1.2 passed all five major crucibles and the bonus test with clarity and visual coherence[cite: 41]. Notably:

- It upheld angular momentum conservation[cite: 42].

- Reproduced lensing and redshift phenomena[cite: 42].

- Modeled quantum analogues via superposition and decoherence[cite: 42].

- Required no dark matter, no scalar fields, and no spacetime curvature[cite: 43].

These results position DWARF not only as a viable alternative to GR but as a potentially more intuitive and empirically versatile framework for understanding gravity, light, and cosmological structure as emergent phenomena from structured flow[cite: 44].